Photoionization of 10-Methylphenothiazine, *N*,*N*,*N*′,*N*′-Tetramethylbenzidine, and Pyrene in Cr−AlMCM-41 Molecular Sieves

Sunsanee Sinlapadech, Ranjit Koodali, R. M. Krishna, and Larry Kevan*

Department of Chemistry, University of Houston, Houston, Texas 77204-5003

Received: January 9, 2002; In Final Form: March 20, 2002

Photoionization of 10-methylphenothiazine (PC_1), *N*,*N*,*N*′,*N*′-tetramethylbenzidine (TMB), and pyrene (Py) impregnated into mesoporous AlMCM-41 ion-exchanged with Cr(III), as an electron acceptor, to give Cr−AlMCM-41 was investigated. Cation radicals ($PC_1^{\bullet+}$, $TMB^{\bullet+}$, $Py^{\bullet+}$) are produced by 320 nm light at room temperature and characterized by electron spin resonance (ESR) and UV−vis diffuse reflectance spectroscopy. The chromium ion concentration was varied from Si/Cr = 52 to 121. Cr−AlMCM-41 with the intermediate concentration of Si/Cr = 80 exhibits the greatest electron acceptor ability and shows the highest photoionization efficiency photoionized. The photoionization efficiency also depends on the type of photoionizable molecule impregnated into mesoporous Cr−AlMCM-41 with PC_1 being the most efficiently photoionized. The calcination temperature used before impregnation controls the oxidation state of chromium ions to Cr^{3+} or Cr^{5+}/Cr^{6+}, which also affects the photoionization efficiency. Cr−AlMCM-41 with Cr^{5+} gives about 4 times higher photoionization efficiency than with Cr^{3+}. Cr−AlMCM-41 is shown to be a promising heterogeneous host for the efficient formation of photoinduced cation radicals to achieve long-lived charge separation in solid-state systems.

Introduction

Photoinduced electron transfer reactions have been extensively studied within the past decade to develop systems for long-lived charge separation, which may be useful for light energy storage. Photosynthesis is a known natural example of photoinduced electron transfer, which converts light energy into usable chemical energy. Light absorption by a chemical system may cause electron transfer from a donor species to an acceptor species, generating a pair of high-energy intermediates that are usually radical ions.[1,2] This charge separation reaction competes with back electron transfer, which must be minimized to maximize the net production of photoproducts. It has been found that radical lifetimes in heterogeneous systems such as micelles,[3−5] vesicles,[6−8] silica gel,[9−12] or zeolites[13,14] are longer than in homogeneous systems. Thus, heterogeneous hosts provide an effective environment to minimize back electron transfer and increase net photoyields.

Recently, MCM-41[15−17] and AlMCM-41[18−20] mesoporous oxide materials have been explored for scientific and industrial applications. MCM-41 or modified MCM-41 materials are able to catalyze some chemical reactions involving large reactants.[21,22] Also, they can be used for selective adsorption of large molecule gases and liquids[23] or heavy metal ions.[24] Prior research has also shown that MCM-41 and AlMCM-41 materials are effective hosts for the net photoionization of incorporated molecules.[25,26] The photoionization efficiency of incorporated molecules in silica and aluminosilica mesoporous materials can be enhanced by also incorporating reducible transition metal ions that act as stable electron acceptors.[25−28]

Transition metal ions such as titanium (Ti^{4+}),[25,26] copper (Cu^{2+}),[29] manganese (Mn^{2+}),[30] or vanadium (V^{5+})[31] have been incorporated into either framework or extraframework (ion-exchange) sites of MCM-41. Previous studies showed that titanium ion (Ti^{4+})[25,26] incorporated into framework sites showed high photoionization efficiency for incorporated photoionizable molecules. Nickel (Ni^{2+}), copper (Cu^{2+}), and iron (Fe^{3+}) ions were also successfully ion-exchanged into AlMCM-41 and enhanced the photoionization of incorporated molecules relative to AlMCM-41 without such ion exchange.[32]

In this work, Cr^{3+} incorporated into AlMCM-41 by ion exchange to form Cr−AlMCM-41 was used as an electron acceptor to enhance photoinduced electron transfer from three different incorporated photoionizable molecules, namely 10-methylphenothiazine (PC_1), *N*,*N*,*N*′,*N*′-tetramethylbenzidine (TMB), and pyrene (Py). The structures, pore sizes, and surface areas of AlMCM-41 with different amounts of Al and Cr were characterized by powder X-ray diffraction and N_2 adsorption. Cr−AlMCM-41 materials were treated at two different temperatures (100 and 550 °C) to vary the oxidation state of chromium. The chromium ion concentration was also varied. The experimental results show that the photoyields can be controlled by the type of photoionizable molecule, the chromium ion content, and the oxidation state of the chromium ions.

Experimental Section

Synthesis of AlMCM-41. Commercial trimethylammonium hydroxide (Aldrich), sodium silicate solution (27 wt % SiO_2; Aldrich), cetyltrimethylammonium bromide (Aldrich), fumed silica (Aldrich), and aluminum nitrate (Aldrich) were used as received for the AlMCM-41 synthesis. MCM-41 and AlMCM-41 materials with different Al contents (Si/Al = 20, 40, and 80) were prepared hydrothermally using cetyltrimethylammonium bromide as the organic template following an earlier procedure.[19]

For MCM-41 synthesis, 10 g of trimethylammonium hydroxide was mixed with 2.95 g of sodium silicate solution and 25 g of distilled water. Cetyltrimethylammonium bromide (4.3 g) was dissolved in 43 g of distilled water, and the solution was slowly

10.1021/jp020020i CCC: $22.00
Published on Web 05/23/2002

added to the mixture. To this mixture was added fumed silica 2.26 g, and the resulting mixture was stirred for 1 h. The pH of the mixture was adjusted to 11.5 using 2 M H_2SO_4. For AlMCM-41 synthesis, 10 g of trimethylammonium hydroxide was mixed with 2.95 g of sodium silicate solution and 10 g of distilled water. Cetyltrimethylammonium bromide (4.3 g) was dissolved in 43 g of distilled water, and the solution was slowly added to the mixture. To this mixture was added fumed silica 2.26 g, and the resulting mixture was stirred for 1 h. Aluminum nitrate (0.96, 0.48 or 0.24 g) was dissolved in 15 g of water, and the solution was added to the mixture. The pH of the mixture was adjusted to 11.5 using 2 M H_2SO_4. All these samples were heated in Teflon bottles for 2 days at about 100 °C. After crystallization, the solid product was filtered out at room temperature. The solid product was washed with distilled water and dehydrated at 80 °C in air for about 3 h. The solid powder is calcined in static air at 550 °C for 12 h to remove water and organic templates.

Characterization. X-ray powder diffraction patterns of AlMCM-41 were obtained with a Philips PW 1840 diffractometer using Cu Kα radiation of wavelength 1.541 Å over the range $1.5° < 2\theta < 15°$. The elemental compositions of AlMCM-41 and Cr−AlMCM-41 were determined with a Kevex 770 X-ray fluorescence spectrometer. A titanium target with an accelerating voltage of 25 kV and a current of 2.5 mA was used for the measurements. The concentrations of the elements were determined by calibration with standards of known concentrations.

Nitrogen adsorption isotherms were measured at 77 K using a Micromeritics Gemini 2375 gas adsorption analyzer. The volume of adsorbed N_2 was normalized to standard pressure and temperature. Prior to the experiments, samples were dehydrated at 280 °C for 3 h. The specific area, A_{BET}, was determined from the linear part of the BET equation. The Barrett−Joyner−Halenda (BJH) method[33] was also used to determine the cumulative pore surface area (A_{BJH}), pore volume (V_{BJH}), and pore sizes (D_{BJH}) of the AlMCM-41 samples. A_{BJH} and V_{BJH} were obtained from the pore size distribution curves, whereas D_{BJH} was calculated from $4V_{BJH}/A_{BJH}$.

The electron spin resonance (ESR) spectra were recorded at room temperature at X-band frequency using a Bruker ESP 300 ESR spectrometer with 100 kHz magnetic field modulation and microwave power low enough to avoid saturation and distortion of the spectrum. The photoproduced $PC_1^{\bullet+}$, $TMB^{\bullet+}$, and $Py^{\bullet+}$ radical yields were determined by double integration of the ESR spectra using the ESP 300 software. The diffuse reflectance (DR) UV−vis spectra were recorded before and after different times of 320 nm photoirradiation at room temperature using a Perkin-Elmer model 330 spectrophotometer with an integrating sphere accessory.

Ion-Exchanged AlMCM-41. $Cr(NO_3)_3 \cdot 9H_2O$ (Aldrich) was used as received for ion exchange. Calcined AlMCM-41 (Si/Al = 20, 40, and 80 gel composition) (1 g) was liquid-state ion-exchanged with 20 mL of 0.1 M chromium ion aqueous solution. The mixture was stirred at room temperature for 24 h. Finally, the material was washed with distilled water and filtered. The chromium ion contents in Cr−AlMCM-41 were determined by X-ray fluorescense (XRF) analysis using a Kevex 770 spectrometer.

Photoionization Samples. 10-Methylphenothiazine (Aldrich), *N*,*N*,*N*′,*N*′-tetramethylbenzidine (Acros), and pyrene (Lancaster) were used as received. AlMCM-41 and Cr−AlMCM-41 were heated at two different temperatures. One set of samples was heated at 100 °C for 3 h to remove water. The second set was heated at 100 °C for 1 h followed by 550 °C for an additional 3 h to remove water and oxidize Cr^{3+} to Cr^{5+}. The solids were impregnated with 10-methylphenothiazine (PC_1), *N*,*N*,*N*′,*N*′-tetramethylbenzidine (TMB), and pyrene (Py) at room temperature by mixing AlMCM-41 or Cr−AlMCM-41 (0.1 g) with 1 mL of 0.01 M PC_1, TMB, or Py in benzene for 1 h in the dark. The benzene was evaporated by flowing dry nitrogen gas over the samples for 30 min. Each sample was transferred into a Suprasil quartz tube (2 mm i.d. × 3 mm o.d.) that was sealed at one end. The sample tube was evacuated below 5 mTorr for 2 h to remove trace amounts of solvent benzene and oxygen and was then flame-sealed for ESR measurements. If evacuation was not done, the photoirradiation results were the same. So it does not appear that trace amounts of these materials, if present, affect the results.

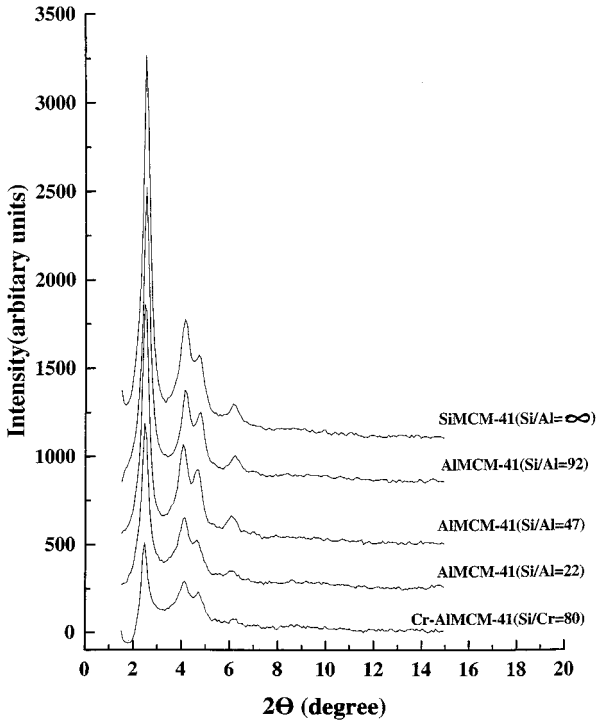

Figure 1. XRD patterns of calcined SiMCM-41, AlMCM-41, and Cr−AlMCM-41.

For diffuse reflectance measurements the samples were filled into a cylindrical quartz sample cell (20 mm diameter by 1 mm path length). AlMCM-41 was used as the reference solid. All samples were handled in the dark to minimize exposure to light.

Each powder was photoirradiated at room temperature with a Cermax 150 W xenon lamp (ILC-LX150 F). The light was passed through a 10 cm water filter and a Corning No. 7-51 glass filter with 90% transparency at 240 and 400 nm and a maximum at 320 nm. The samples were rotated during photoirridiation for uniform exposure to the light. Electron spin resonance was used to detect the photoproduced cation radicals. The cation radical yield ($PC_1^{\bullet+}$, $TMB^{\bullet+}$, $Py^{\bullet+}$) produced from the reaction was determined by ESR and by diffuse reflectance UV−vis spectroscopy.

Results

XRD and N_2 Adsorption. The XRD patterns of calcined siliceous MCM-41, AlMCM-41 with different Si/Al ratios and Cr−AlMCM-41 are consistent with previous reports,[15,16,32] as shown in Figure 1. No impurity phase was detected. The well-defined reflections at 100, 110, 200, and 210 indicate a hexagonal structure for these materials. Table 1 shows the BET

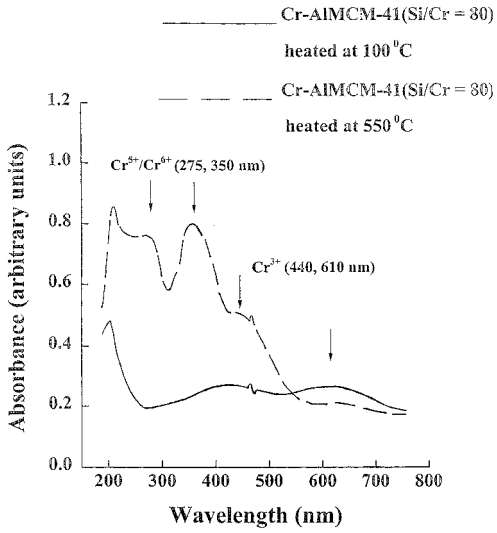

Figure 2. UV−vis diffuse reflectance spectra (DRS) at room temperature of Cr−AlMCM-41(Si/Cr=80) heated at 100 and at 550 °C.

TABLE 1: Pore Structure Parameters of AlMCM-41 Calculated from the Adsorption Branch of Nitrogen Adsorption Isotherms

materials	A_{BET} ($m^2\ g^{-1}$)	A_{BJH} ($m^2\ g^{-1}$)	D_{BJH} (Å)	V_{BJH} ($cm^3\ g^{-1}$)
SiMCM-41 (Si/Al = ∞)	1021	1112	29	0.9
AlMCM-41 (Si/Al = 92)	1017	1105	31	0.9
AlMCM-41 (Si/Al =47)	912	967	35	0.9
AlMCM-41 (Si/Al = 22)	850	916	41	1.0
Cr−AlMCM-41 (Si/Al = 92) (Si/Cr = 121)	871	914	31	0.7
Cr−AlMCM-41 (Si/Al = 47) (Si/Cr = 80)	819	745	36	0.6
Cr−AlMCM-41 (Si/Al = 22) (Si/Cr = 52)	682	553	41	0.5

surface areas (A_{BET}), BJH surface areas (A_{BJH}), volume absorbed (V_{BJH}), and pore sizes (D_{BJH}) of MCM-41, AlMCM-41, and Cr−AlMCM-41 with different Al or Cr contents. The adsorption isotherm exhibits a large increase in the P/P_0 range from 0.2 to 0.3, characteristic of capillary condensation in MCM-41 mesopore materials.[18,34] Increasing the Al content in AlMCM-41 results in a small decrease of the A_{BET} surface area. However, the pore sizes (D_{BJH}) for different Si/Al ratios in AlMCM-41 are similar. This confirms that the AlMCM-41 materials are still mesoporous. After AlMCM-41 is ion-exchanged with Cr^{3+}, all A_{BET} areas are significantly reduced by about 10−20%, which seems to indicate some structural degradation. The elemental composition of AlMCM-41 and Cr−AlMCM-41 were done by XRF. Comparison between the gel composition Si/Al ratio and the elemental ratio from XRF from the AlMCM-41 product are similar (20 gel versus 22 product, 40 gel versus 47 product, and 80 gel versus 92 product).

UV−Vis and ESR of Cr−AlMCM-41. Figure 2 shows UV−vis spectra of Cr−AlMCM-41(Si/Al=47)(Si/Cr=80) heated at 100 °C for 3 h or at 550 °C for 3 h. For 100 °C heating, two broad peaks at 440 and 610 nm characteristic of Cr^{3+} are observed. These peaks can be assigned to d−d transitions described as $^4A_{2g} \rightarrow {}^4T_{2g}$ and $^4A_{2g} \rightarrow {}^4T_{1g}$.[35,36] The small sharp shoulder at 465 nm can be assigned to a spin-forbidden $^4A_{2g} \rightarrow {}^2T_{2g}$ transition.[35,37] When the sample is heated at 550 °C, Cr^{3+} is oxidized to Cr^{5+} and/or Cr^{6+}. As one can see from Figure 2, the UV−vis spectrum of Cr−AlMCM-41 heated to 550 °C shows bands at 275 and 350 nm, a shoulder around 440 nm and a very weak band around 610 nm. The bands at 275 and 350 nm are normally assigned to $O \rightarrow Cr^{6+}$ charge-transfer absorption bands.[35,37,38] However, the d−d transition of Cr^{5+} occurs in the same spectral region.[39] ESR results show that some Cr^{5+} is present in the sample after calcination. Thus, the bands observed in the ultraviolet region may be due to the overlap of a Cr^{5+} d−d transition and an $O \rightarrow Cr^{6+}$ charge-transfer band, although the Cr^{6+} band is probably more intense. The two bands at 440 and 610 nm can be assigned to octahedral Cr^{3+} ions, implying that there is a small amount of unoxidized Cr^{3+} even after heating at 550 °C.[40] However, the band at 440 nm is also characteristic of a forbidden charge-transfer band of dichromate-like spectra.[36] Thus the band at 440 nm is likely a superposition of two contributions.

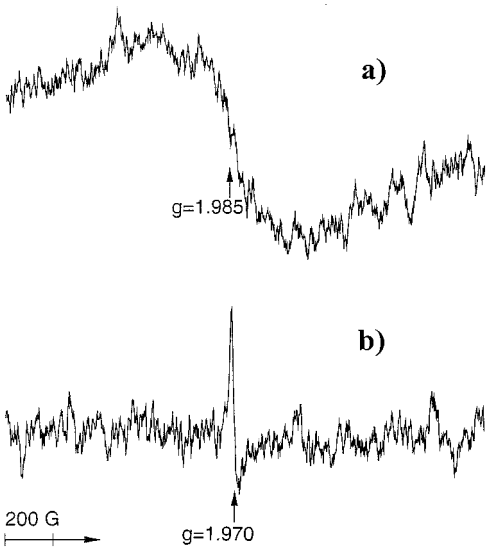

Figure 3. ESR spectra at room temperature of Cr−AlMCM-41(Si/Cr=80) heated at (a) 100 °C and (b) 550 °C for 3 h.

Parts a and b of Figure 3 show ESR spectra of Cr−AlMCM-41(Si/Al=47)(Sr/Cr=80) heated in air at (a) 100 °C for 3 h and (b) 550 °C for 3 h. In Figure 3a, a broad line of Cr^{3+} appears at $g = 1.985$. After heating at 550 °C, the signal of Cr^{3+} disappears and a sharp line of Cr^{5+} appears at $g = 1.970$. These results are similar to those of a previous study on CrMCM-41.[35] It is found that the ESR intensities of Cr^{3+} and Cr^{5+} increase as the amount of chromium ion increases but that the line width remains the same (not shown). Since Cr^{6+} is ESR silent, the g value, line width, and line shape of Cr^{5+} in Cr−AlMCM-41 at room temperature suggest that Cr^{5+} is present in either square-pyramidal or distorted octahedral coordination, where the additional coordination is due to water.[41] These two differently heated samples were irradiated with 320 nm light at room temperature for 60 min in order to assess the stability of these materials without incorporated photoionizable species. No significant change is observed.

Photoionization of Electron Donor Organic Molecules in MCM-41, AlMCM-41, and Cr−AlMCM-41. 10-Methylphenothiazine (PC_1),[11,26,27,32] *N*,*N*,*N*′,*N*′ tetramethylbenzidine (TMB),[14,42] and pyrene (Py)[43,44] can be photoionized to produce cation radicals. The sizes of PC_1, TMB, and Py are about 6.5 Å × 10 Å, 5 Å × 13 Å, and 6.9 Å × 10 Å, respectively. This means that the 30 Å or larger channel openings of mesoporous MCM-41 materials should be big enough to incorporate these electron donor species. Incorporation of 10-methylphenothiazine

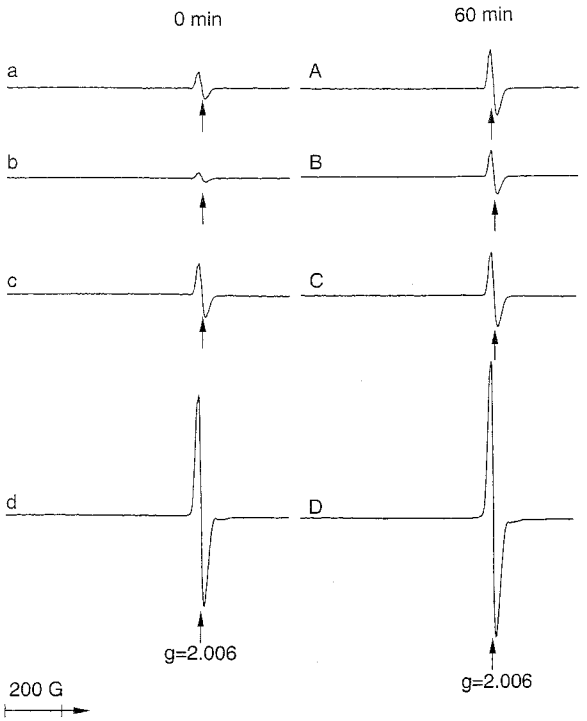

Figure 4. ESR spectra of $PC_1^{\bullet+}$ in AlMCM-41/PC_1 (a-A) heated at 100 °C and (b-B) heated at 550 °C and in Cr−AlMCM-41/PC_1 (c-C) heated at 100 °C and (d-D) heated at 550 °C at 0 and 60 min irradiation time with 320 nm light at room temperature.

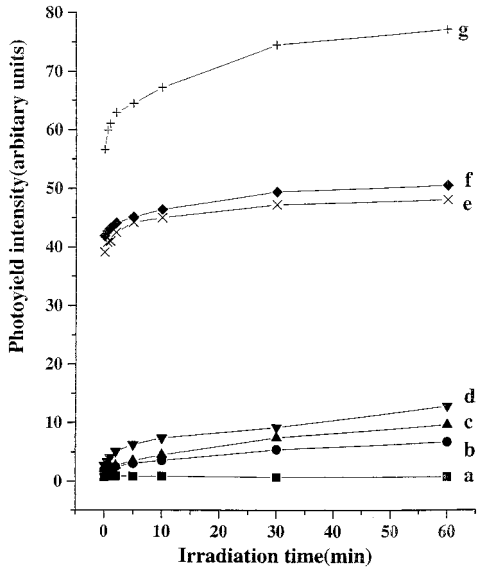

Figure 5. ESR intensity of $PC_1^{\bullet+}$ in (a) MCM-41/PC_1, (b) AlMCM-41(Si/Al=22)/PC_1, (c) AlMCM-41(Si/Al=47)/PC_1, (d) AlMCM-41-(Si/Al=92)/PC_1, (e) Cr−AlMCM-41(Si/Cr=121)/PC_1, (f) Cr−AlMCM-41(Si/Cr=52)/PC_1, and (g) Cr−AlMCM-41(Si/Cr=80)/PC_1 versus 320 nm irradiation time at room temperature.

(PC_1) into AlMCM-41 and Cr−AlMCM-41 produces a thermally produced (dark reaction) ESR signal of methylphenothiazine cation radicals ($PC_1^{\bullet+}$) as shown in Figure 4. The samples are light pink before irradiation (a−d) and turn darker pink after 60 min irradiation (A−D). The pink color is characteristic of $PC_1^{\bullet+}$ cation radicals.[26,27,32] The unresolved signal with a g value of 2.006 is assigned to $PC_1^{\bullet+}$ following previous literature.[26,27,32] Interestingly, the dark reaction for AlMCM-41 is less when it is heated at 550 °C before impregnation as shown in Figure 4a,b. This suggests that some surface hydroxyl groups, which may possibly act as electron acceptors,[9] are removed by heating, causing less dark reaction. In contrast, the dark reaction of Cr−AlMCM-41 is much larger than for AlMCM-41 and is especially so after heating at 550 °C before impregnation as shown in Figure 4c,d. This must be due to the oxidation of most Cr^{3+} (at 100 °C) to Cr^{5+}/Cr^{6+} (at 550 °C), which is a better electron acceptor as indicated by their reduction potentials, $E°(Cr^{5+}/Cr^{4+}) = 1.340$ V and $E°(Cr^{3+}/Cr^{2+}) = -0.407$ V.[45] It is clear from the spectra that PC_1 is photoionized to its radical form $PC_1^{\bullet+}$ by 320 nm light at room temperature. All samples show a photoyield intensity increase after irradiating by 320 nm light at room temperature for 60 min. A very small signal of $PC_1^{\bullet+}$ in MCM-41/PC_1 (not shown) before and after irradiation is also observed, but the ESR spectrum is unchanged after 60 min irradiation.

Figure 5 shows photoyield intensities of $PC_1^{\bullet+}$ in MCM-41/PC_1, AlMCM-41/PC_1 for different Si/Al ratios, and Cr−AlMCM-41/PC_1 for different Si/Cr ratios. The photoyield intensities are lower for MCM-41/PC_1 and AlMCM-41/PC_1 at different Si/Al ratios and are higher for Cr−AlMCM-41/PC_1 at different Si/Cr ratios. The Cr materials show a larger dark reaction and larger photoyield intensity increases. This implies that Cr−AlMCM-41 provides a better system for charge separation than MCM-41 and AlMCM-41, although it is definitely desirable to minimize the dark reaction. After being irradiated with 320 nm light at room temperature for 60 min, the photoyield intensity of $PC_1^{\bullet+}$ in MCM-41/PC_1 is unchanged but AlMCM-41/PC_1 and Cr−AlMCM-41/PC_1 show increases. For AlMCM-41, the net photoyield intensities increase by 4.7, 7.5, and 10.1 units for Si/Al = 22, 47, and 92, respectively. The greater the aluminum content, the less is the net photoyield increase. This is not true for the Cr−AlMCM-41 samples. The net photoyield intensities increase by 8.5, 20.4, and 8.9 units for Si/Cr = 52, Si/Cr = 80, and Si/Cr = 121, respectively. There is an optimum concentration for the photoyield increase in the Cr−AlMCM-41/PC_1 samples. The yields of $PC_1^{\bullet+}$ in MCM-41/PC_1, AlMCM-41/PC_1, and Cr−AlMCM-41/PC_1 slowly decrease during the first 24 h after photoirradiation and then are relatively stable for several days.

ESR spectra of Cr−AlMCM-41(Si/Cr=80) impregnated with pyrene (Py; Figure 6a-6A), *N*,*N*,*N*′,*N*′-tetramethylbenzidine (TMB; Figure 6b-6B), and 10-methylphenothiazine (PC_1; Figure 6c-6C) are shown. All these samples were heated at 100 °C for 3 h before impregnation to remove water. The results show that some $Py^{\bullet+}$, $TMB^{\bullet+}$, and $PC_1^{\bullet+}$ are produced thermally (dark reaction) at $g = 2.006$ before 320 nm light irradiation. These radical intensities increase 0.4, 3.0, and 5.7 units for Cr−AlMCM-41/Py, Cr−AlMCM-41/TMB, and Cr−AlMCM-41/PC_1, respectively, after 60 min photoirradiation. Similar experiments were done after heating Cr−AlMCM-41 samples at 550 °C for 3 h before impregnation, which oxidizes Cr^{3+} to Cr^{5+}/Cr^{6+}. ESR spectra of the samples heated to 550 °C are shown in Figure 7. One can clearly distinguish the Cr^{5+} ESR signal at $g = 1.974$ from that of the cation radical ions at $g = 2.006$ in Cr−AlMCM-41/Py but much less so in Cr−AlMCM-41/TMB and Cr−AlMCM-41/PC_1. This is because the peak-to-peak line width of $Py^{\bullet+}$ (10 G) is significantly smaller than those of $TMB^{\bullet+}$ (24 G) or $PC_1^{\bullet+}$ (28 G). These radical intensities increase 0.2 units for Cr−AlMCM-41/Py and 20.4 units for Cr−AlMCM-41/PC_1 but decrease 3.3 units for Cr−AlMCM-41/TMB after 60 min of photoirradiation. Unfortunately, we cannot accurately measure the changing concentration of Cr^{5+} in Cr−AlMCM-41/Py because the signal difference between 0 and 60 min photoirradiation is too small. Also, we cannot determine the concentration change of Cr^{5+} in Cr−AlMCM-41/PC_1 and Cr−AlMCM-41/TMB since the signals of Cr^{5+} and the organic

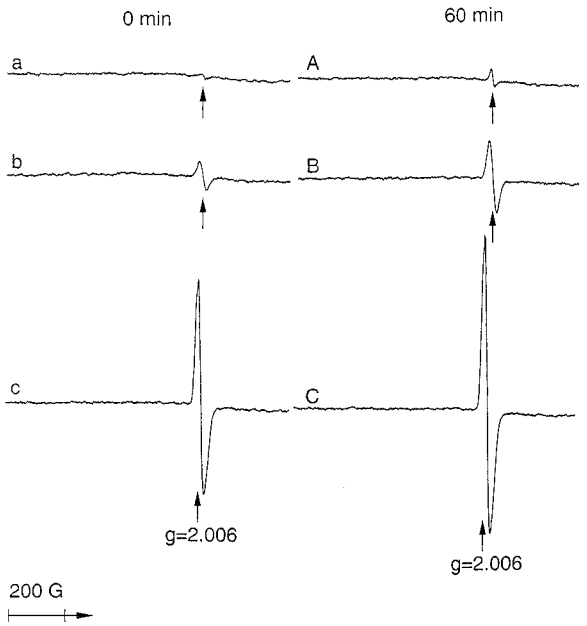

Figure 6. ESR spectra of (a) $Py^{\bullet+}$ in Cr−AlMCM-41/Py, (b) $TMB^{\bullet+}$ in Cr−AlMCM-41/TMB, and (c) $PC_1^{\bullet+}$ in Cr−AlMCM-41/PC_1 at 0 (a−c) and 60 (A−C) min irradiation time with 320 nm light at room temperature. Cr−AlMCM-41(Si/Cr=80) is heated at 100 °C before incorporating the donor molecules.

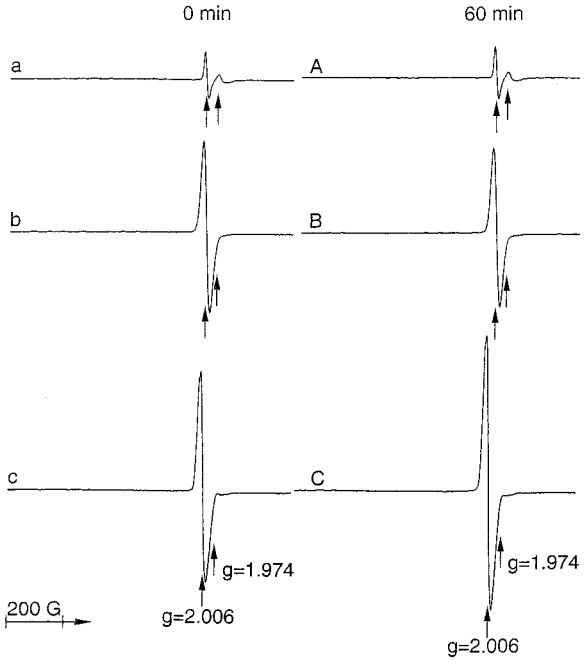

Figure 7. ESR spectra of (a) $Py^{\bullet+}$ in Cr−AlMCM-41/Py, (b) $TMB^{\bullet+}$ in Cr−AlMCM-41/TMB, and (c) $PC_1^{\bullet+}$ in Cr−AlMCM-41/PC_1 at 0 (a−c) and 60 (A−C) min irradiation time with 320 nm light at room temperature. Cr−AlMCM-41(Si/Cr=80) is heated at 550 °C before incorporating the donor molecules.

radicals ($PC_1^{\bullet+}$ and $TMB^{\bullet+}$) overlap each other too much. The photoyield intensities for Cr−AlMCM-41/Py and Cr−AlMCM-41/TMB heated to 550 °C are not much changed after photoirradiation. Therefore, we presume that the dark reactions for these two systems are comparable to their maximum photoionization efficiencies. The photoionization efficiency of the samples heated to 100 and 550 °C may be compared for PC_1 since it gives the greatest photoyield increase among the three organic donor molecules after 60 min photoirradiation. It is evident that $PC_1^{\bullet+}$ has a higher yield in Cr−AlMCM-41

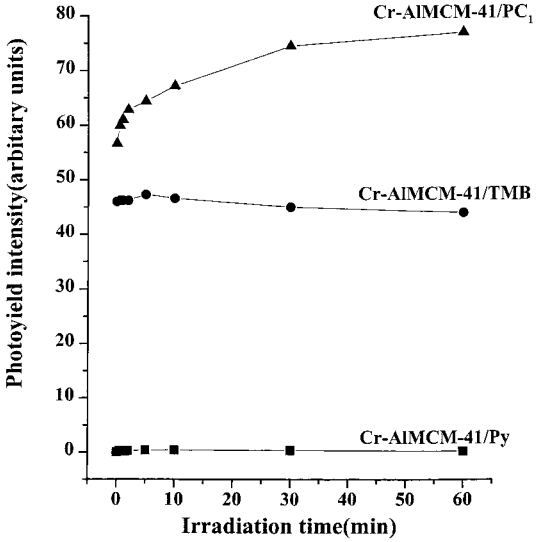

Figure 8. ESR intensity of $PC_1^{\bullet+}$, $TMB^{\bullet+}$, and $Py^{\bullet+}$ cation radicals in Cr−AlMCM-41(Si/Cr=80)/PC_1 or TMB or Py versus 320 nm irradiation time at room temperature. Cr−AlMCM-41 is heated at 550 °C before incorporating the donor molecules.

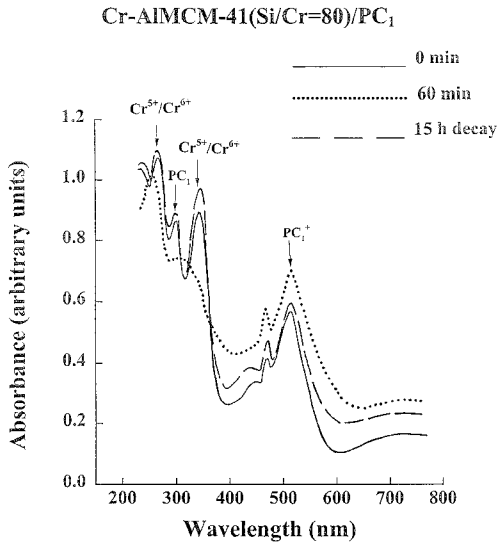

Figure 9. UV−vis diffuse reflectance spectra at room temperature of Cr−AlMCM-41(Si/Cr=80)/PC_1 at 0 and 60 min irradiation time with 320 nm light at room temperature and at 15 h after photoirradiation. Cr−AlMCM-41 is heated at 550 °C before incorporating the donor molecules.

heated at 550 °C (20.4 units increase) than when heated at 100 °C (only 5.7 units increase). The photoyield intensities of the cation radicals in Cr−AlMCM-41 samples heated to 550 °C are plotted in Figure 8. The dark reaction becomes less as the size of the electron donor species increases. Cr−AlMCM-41/PC_1 exhibits a photoyield increase when irradiated by 320 nm light for 60 min, whereas Cr−AlMCM-41/TMB shows a small photoyield increase only for the first 5 min before subsequently decreasing and Cr−AlMCM-41/Py shows no photoyield increase. A decrease of $TMB^{\bullet+}$ during photoirradiation may be due to generation of some nonparamagnetic TMB_2^{2+}.[14] After 24 h after photoirradiation the photoyield intensity decreases 23% for Cr−AlMCM-41/Py, 33% for Cr−AlMCM-41/TMB and only 7% for Cr−AlMCM-41/PC_1.

Diffuse UV−vis spectra of Cr−AlMCM-41(Si/Al=47)(Si/Cr=80) /PC_1 are shown in Figure 9. The pink color characteristic of $PC_1^{\bullet+}$ cation radicals[26,27,32] is also observed before irradiation and shows absorption in the visible range (515 nm). This also

supports that some PC_1 is ionized to $PC_1^{\bullet+}$ thermally during sample preparation. From Figure 9, when Cr−AlMCM-41/PC_1 is irradiated by 320 nm light for 60 min, the $PC_1^{\bullet+}$ photoyield significantly increases while the absorption of PC_1 decreases and also the two absorption peaks at 275 and 350 nm assigned to Cr^{5+}/Cr^{6+}decrease. This shows that there is electron transfer from PC_1 to Cr^{5+}/Cr^{6+} during photoirradiation.

Further study was focused on the effect of the chromium amount in Cr−AlMCM-41 on the photoyield. The photoyield of $PC_1^{\bullet+}$ increases with increasing irradiation time. The maximum net photoyield increase was obtained for Si/Cr = 80. At low Cr content (Si/Cr = 121), the photoyield seems rather constant after 10 min photoirradiation at room temperature. For higher Cr content (Si/Cr = 52), the photoyield increases after 10 min of photoirradiation and reaches a plateau after about 30 min. However, the net photoyield intensity increase after 10 min photoirradiation for Si/Cr = 80 is larger than that for Si/Cr = 52. After 60 min irradiation, the photoyield intensities of $PC_1^{\bullet+}$ in Cr−AlMCM-41/PC_1 increased 23% for Si/Cr = 121, 36% for Si/Cr = 80, and 20% for Si/Cr = 52.

Discussion

XRD and N_2 adsorption experiments indicate that the cage sizes of AlMCM-41 are large enough to incorporate 10-methylphenothiazine (PC_1), *N*,*N*,*N*′,*N*′-tetramethylbenzidine (TMB), and pyrene (Py). ESR and diffuse reflectance UV−vis spectra of some 10-methylphenothiazine cation radicals (g = 2.006 for ESR or 515 nm for DRS) were observed after sample preparation and before photoirradiation. This indicates that the impregnation procedure for PC_1 into AlMCM-41 thermally oxidizes some of the PC_1 into $PC_1^{\bullet+}$.[25,26,32] This is also true of TMB and Py since ESR signals of $TMB^{\bullet+}$ and $Py^{\bullet+}$ at g = 2.006 are likewise observed after sample preparation.

The effect of heating Cr−AlMCM-41 before impregnation with PC_1, TMB, or Py on the photoionization efficiency is considerable. Heating to 550 °C before impregnation causes the oxidation of Cr^{3+} to Cr^{5+}/Cr^{6+}. Cr^{5+} is a better electron acceptor according to its reduction potential. This fact is consistent with the ESR results where the net photoyield of $PC_1^{\bullet+}$ in Cr−AlMCM-41/PC_1 heated at 550 °C is about 4 times greater than when heated at 100 °C where the Cr ion still exists as Cr^{3+}.

The photoionization efficiency clearly depends on the type of incorporated photoionizable molecule. Among the three different organic molecules studied, PC_1 is the best electron donor with the highest net photoyield intensity and also the longest radical lifetime. The high photoionization efficiency of PC_1 is not explained by the ionization potentials determined by photoelectron spectroscopy, which are PC_1 (7.15 eV[46]), TMB (6.84 eV[47]), and Py (7.45 eV[48]). The expected order of photoyields based on the ionization potentials is Cr−AlMCM-41/TMB > Cr−AlMCM-41/PC_1 > Cr−AlMCM-41/Py. However, the observed order is Cr−AlMCM-41/PC_1 > Cr−AlMCM-41/TMB > Cr−AlMCM-41/Py. The higher ionization potential of pyrene may explain its low photoyield. The low photoyield of $TMB^{\bullet+}$ may be due to the formation of some nonparamagnetic $(TMB)_2^{2+}$.[14,32] In addition, the photoionization efficiency depends on the stability of the photoproduced radical cations. It is found that $TMB^{\bullet+}$ and $Py^{\bullet+}$ decay 33% and 23%, respectively, compared to only 7% for $PC_1^{\bullet+}$ in 24 h.

The photoyield of $PC_1^{\bullet+}$ increases in the order MCM-41 < AlMCM-41 < Cr−AlMCM-41, indicating that the chromium ion in Cr−AlMCM-41 enhances the photoionization reaction. We previously found that the concentration of Ni^{2+} ion-exchanged into AlMCM-41 enhanced the photoyield of incorporated photoionizable molecules.[32] The photoyield in Cr−AlMCM-41/PC_1 initially increases with the amount of Cr^{3+} ion-exchanged into AlMCM-41. However, for Si/Cr = 52 the photoyield decreases. This may be explained by some structural degradation at higher Cr content and/or by the formation of secondary radicals.[9,14] Therefore, the amount of Cr ions ion-exchanged into extraframework sites of AlMCM-41 has an optimal value to achieve maximum charge separation. One can also conclude that Cr^{5+}/Cr^{6+} in Cr−AlMCM-41 enhances charge separation by accepting an electron from the electron donor species, as illustrated in Figure 9. The optical spectra support that electron transfer occurs between PC_1 and Cr^{5+}/Cr^{6+}. In Cr−AlMCM-41/PC_1 calcined at 100 °C, the bands due to Cr^{3+} and $PC_1^{\bullet+}$ overlap in the region 440−600 nm and do not clearly indicate the nature of electron trapping sites in Cr−AlMCM-41 calcined at 100 °C.

Incorporation of Al into the MCM-41 framework creates Lewis and Bronsted acid sites.[19] As plotted in Figure 5, the more Al in AlMCM-41/PC_1, the less the net photoyield. For AlMCM-41, the hydroxyl groups of the framework may serve as electron acceptors with production of hydrogen atoms. However, no ESR signals due to trapped hydrogen atoms were detected. This is consistent with an earlier report in which trapped hydrogen atoms were not observed in material having pore sizes similar to the one in the present study.[9]

Conclusions

ESR and UV−vis spectroscopies were used to study photoionization of 10-methylphenothiazine (PC_1), *N*,*N*,*N*′,*N*′-tetramethylbenzidine (TMB) and pyrene (Py) in Cr−AlMCM-41 mesoporous materials. It is found that PC_1 incorporated into Cr−AlMCM-41 is the best electron donor among these three photoionizable molecules. Formation of cation radicals within modified Cr−AlMCM-41 materials is due to electron transfer between the electron donor molecules and chromium ions, with Cr^{5+}/Cr^{6+} being a better electron acceptor than Cr^{3+}. It is verified that the photoyield intensity depends on the amount of chromium ions ion-exchanged into the mesoporous AlMCM-41 materials, but an intermediate concentration is optimal. The temperature before impregnation controls the chromium ion valence state and the photoyield. Also the photoyield depends of the type of photoionizable molecule.

Acknowledgment. This research was support by the Division of Chemical Sciences, Office of Basic Energy Sciences, Office of Energy Research, U.S. Department of Energy, the Texas Advanced Research Program and the Environmental Institute of Houston.

References and Notes

(1) Kavarnos, G. J.; Turro, N. J. *Chem. Rev.* **1986**, *86*, 401.
(2) Seava, F. D. *Top. Curr. Chem.* **1990**, *156*, 60.
(3) Vermeulen, L. A.; Thompson, M. E. *Nature* **1992**, *358*, 656.
(4) Nakato, T.; Kazuyuki, K.; Koto, C. *Chem. Mater.* **1992**, *4*, 128.
(5) Baglioni, P.; Hu, M.; Kevan, L. *J. Phys. Chem.* **1990**, *94*, 2586.
(6) Kang, Y. S.; McManus, H. J. D.; Kevan, L. *J. Phys. Chem.* **1993**, *97*, 2027.
(7) Kurshev, V.; Kevan, L. *Langmuir* **1997**, *13*, 225.
(8) Jung, J.-A.; Shin, D. R.; Kim, J.-S.; Kang, Y. S.; Kevan, L. *J. Chem. Soc., Faraday Trans.* **1998**, *94* (11), 1619.
(9) Xiang, B.; Kevan, L. *Langmuir* **1994**, *10*, 2688.
(10) Xiang, B.; Kevan, L. *J. Phys. Chem.* **1994**, *98*, 5120.
(11) Xiang, B.; Kevan, L. *Langmuir* **1995**, *11*, 860.
(12) Sung-Suh, H. M.; Kevan, L. *J. Chem. Soc., Faraday Trans.* **1998**, *94* (10), 417.
(13) Ledney, M.; Dutta, P. K. *J. Am. Chem. Soc.* **1995**, *117*, 7687.
(14) Koodali, T. R.; Kevan, L. *Phys. Chem. Chem. Phys.* **2001**, *3*, 2921.

(15) Kresge, C. T.; Leonowicz, W. J.; Roth, W. J.; Vartuti, J. C.; Beck, J. S. *Nature* **1992**, *359*, 710.

(16) Beck, J. S.; Vartuli, J. C.; Roth, W. J.; Leonowicz, M. E.; Kresge, C. T.; Schmitt, K. D.; Chu, C. T.; Olson, D. H.; Sheppard, E. W.; McCulley, S. B.; Higging, J. B.; Schlenker, J. L. *J. Am. Chem. Soc.* **1992**, *114*, 10834.

(17) Ying, J. Y.; Mehnert, C. P.; Wong, M. S. *Angew. Chem., Int. Ed. Engl.* **1999**, *38*, 56.

(18) Boger, T.; Roesky, R.; Gläser, R.; Ernst, S.; Eigenberger, G.; Weitkamp, J. *Micropor. Mater.* **1997**, *8*, 79.

(19) Luan, Z.; Cheng, C.-F.; Zhou, W.; Klinowski, J. *J. Phys. Chem.* **1995**, *99*, 1018.

(20) Biz, S.; White, M. G. *J. Phys. Chem. B* **1999**, *103*, 8432.

(21) Corma, A.; Navarro, M. T.; Pariente, J. P. *J. Chem. Soc., Chem. Commun.* **1994**, 147.

(22) Reddy, K. M.; Song, C. *Catal. Lett.* **1996**, *36*, 103.

(23) Ioneva, M. A.; Newman, G. K.; Harwell, J. H. *AIChE Symp. Ser.* **1995**, *91* (3), 40.

(24) Feng, X.; Fryxell, G. E.; Wang, L.-Q.; Kim, A. Y.; Liu, J.; Kemmer, K. M. *Science* **1997**, *276*, 923.

(25) Sung-Suh, H. M.; Luan, Z.; Kevan, L. *J. Phys. Chem. B* **1997**, *101*, 10455.

(26) Krishna, R. M.; Prakash, A. M.; Kevan, L. *J. Phys. Chem. B* **2000**, *104*, 1796.

(27) Kurshev, V.; Prakash, A. M.; Krishna, R. M.; Kevan, L. *Micropor. Mesopor. Mater.* **2000**, *34*, 9.

(28) Koodali, T. R.; Chang, Z.; Krishna, R. M.; Prakash, A. M.; Kevan, L. *J. Phys. Chem. B* **2000**, *104*, 5579.

(29) Luan, Z.; Xu, J.; Kevan, L. *Nukleonika* **1997**, *42*, 493.

(30) Xu, J.; Luan, Z., Wasowicz, T.; Kevan, L. *Micropor. Mesopor. Mater.* **1998**, *22*, 179.

(31) Luan, Z.; Xu, J.; He, H.; Klinowski, J.; Kevan, L. *J. Phys. Chem.* **1996**, *100*, 19595.

(32) Sinlapadech, S.; Krishna, R. M.; Luan, Z.; Kevan, L. *J. Phys. Chem. B* **2001**, *105*, 4350.

(33) Barrett, E. P., Joyner, L. G.; Halenda, P. P. *J. Am. Chem. Soc.* **1951**, *73*, 373.

(34) Sing, K. S. W.; Everett, D. H.; Haul, R. A. W.; Moscow, L.; Pierotti, R. A.; Rouquerol, J.; Siemieniewska, T. *Pure Appl. Chem.* **1985**,*57*, 603.

(35) Zhu, Z.; Chang, Z.; Kevan, L. *J. Phys. Chem. B* **1999**, *103*, 2680.

(36) (a) Weckhuysen, B. M.; Wachs, I. E.; Schoonheydt, R. A. *Chem. Rev.* **1996**, *96*, 3327. (b) Weckhuysen, B. M.; Rao, R. R.; Pelgrims, J.; Schoonheydt, R. A.; Bodart, P.; Debras, G.; Collart, O.; Van Der Voort, P.; Vansant, E. F. *Chem. Eur. J.* **2000**, *6*, 2960.

(37) McCarthy, P.; Lauffenburger, J.; Skonezny, P. Pohrer, D. *Inorg. Chem.* **1981**, *20*, 1566.

(38) Mambrim, J. S. T.; Pastore, H. O.; Davanzo, C. U.; Vichi, E. J. S.; Nakamura, O.; Vagus, H. *Chem. Mater.* **1993**, *5*, 166.

(39) Garner, C. D.; Kendrick, J.; Lambert, P.; Mabbs, F. E.; Hillier, I. H. *Inorg. Chem.* **1976**, *15*, 1287.

(40) Yuan, Z. Y.; Wang, J. Z.; Zhang, Z. L.; Chen, T. H.; Li, H. X. *Micropor. Mesopor. Mater.* **2001**, *43*, 227.

(41) Zhu, Z.; Wasowicz, T.; Kevan, L. *J. Phys. Chem. B* **1997**, *101*, 10163.

(42) Krishna, R. M.; Kevan, L. *Micropor. Mesopor. Mater.* **1999**, *32*, 169.

(43) Liu, X.; Iu, K.-K.; Thomas, J. K. *J. Phys. Chem.* **1989**, *93*, 4120.

(44) Pankasem, S.; Thomas, J. K. *J. Phys. Chem.* **1991**, *95*, 6990.

(45) *Handbook of Chemistry and Physics*, 80th ed.; Lide, D. R., Ed.; CRC Press: Boca Raton, FL, 1999; pp 8−22.

(46) Domelsmith, L. N.; Munchausen, L. L.; Houk, K. N. *J. Am. Chem. Soc.* **1977**, *99*, 6506.

(47) Ballard, R.E.; Kones, J.; Read, D.; Inchley, A.; Cranmer, M. *Chem. Phys. Lett.* **1987**, *137*, 125.

(48) Dewar, M. J. S.; Goodman, D.W. *J. Chem. Soc., Faraday Trans.* **1972**, *68*, 1748.